I R A N INTERNATIONAL ALUMINIUM CONFERENCE

IIAC 2012

This certificate is awarded for paper entitled as;

Numerical Investigation of the Effects of Constraint Design on 5XXX Al Alloy GTA Welding

Authored by;

M. Shateryan, A. Rezaee-Bazzaz, M. Haddad Sabzevar, B. Naderi

which was presented in

Iran International Aluminium Conference 2012

مرکز تحقیقات آلومینیوم ایران
Iran Aluminium Research Centre

IMIDRO
Iranian Mines and Mineral Industries Development and Renovation Organization

Chairman

Prof. M. R. Aboutalebi

Scientific Chairman

Dr. M. Soltanieh

Proceedings of Iran International Aluminum Conference (IIAC2012)
May 15-16, 2012, Arak, I.R. Iran

Numerical investigation of the effects of constraint design on 5XXX Al Alloy GTA Welding

Mohsen Shateryan[a,*], Abolfazl Rezaee-Bazzaz[a], Mohsen Haddad Sabzevar[a], Behroz Naderi [b]

[a] Department of Material Engineering, Faculty of Engineering Ferdowsi University of Mashhad, Mashhad, P.O. Box: 9177948974, Iran

Abstract: One of the most conventional approaches of quality control in metal weldments is the evaluation of residual stresses and distortion. Constraining the structure during welding, is the significant key parameter for optimizing the residual stress. In this research, an attempt was made to obtain the best welding constraint of 5XXX Al alloy lap joints during double pass GTAW. A 3-Dimentional finite element simulation was utilized for determining the effect of three different types of local U-shape Fixture (LUF) on residual stresses distributions and distortion. Considering sequentially coupled thermal-mechanical strategy, double ellipsoidal modelling of heat source and element death and birth technique were used in simulation. Thermocouple and LVDT's set up were applied to validate thermal and mechanical results, respectively. Results provided by simulation show acceptable agreement with experimental values. According to results obtained from simulation, suitable LUFs selected based on optimum residual stresses and distortion in welding the aluminium structure.

Keywords: GTA welding; Residual stress; Numerical analysis; Distortion

Introduction

Al-alloy structures are increasingly used for many applications such as shipbuilding, petroleum storage, railway vehicles, bridges, automotive and aerospace industries. They offer lightweight construction with maximum efficiency and reliability[1]. However, the majority of Al-alloys structures show critical points in welded connections, mainly when they are subjected to cyclic loading. The highly localized transient heat and strongly nonlinear temperature fields in both heating and cooling processes cause nonuniform thermal expansion and contraction, and thus result in plastic deformation in the weld and surrounding areas. As a result, residual stress, strain and distortion are permanently produced in the welded structures. High tensile residual stresses are known to promote fracture and fatigue, while compressive residual stresses may induce undesired, and often unpredictable, global or local buckling during or after the welding[2]. This distortion is particularly evident with large and thin panels, as used in the construction of automobile bodies and ships.

In aluminum structures welding for the shipbuilding industry, the main objective is to minimize distortion to avoid fit-up problems in production of the final assembly. Also maximizing the strength of the heat affected zone (HAZ) of the weld is highly concerned about. Finally, the welding residual stresses should be quantified to achieve a safe design with reliable failure assessment. Using mechanical constraint, like fixtures, during the welding is a method to control the residual stress and distortions. Appropriate installing fixture before welding sequence facilitates production of a weld with good conditions. Suitable fixtures decrease the residual stress magnitudes, while excessive constraint by improper fixture condition caused to produce unexpected distortion due to heat flux in welding. These adversely affect the fabrication, assembly and service life of the structures. Therefore the knowledge of the residual stress state, both qualitatively and quantitatively is highly interested. This knowledge would also permit more rational and precise use of the stress-relief techniques.

Over the past decades, considerable investigations have been conducted for the use of advanced analytical procedures to more accurately simulate the welding process. Due to complexity of physical processes involved in welding, simple mathematical equations for describing the residual stress and distortion distribution in the practical manufacturing processes cannot be obtained. Computational simulation, thus plays an indispensable role in the integrity analysis of such welded structures[3]. Hibbitt and Sherief [4-5] applied a two-dimensional (2D) finite element analysis (FEA) to predict residual stresses in a welding for the first time. Due to computational and cost limitations, FEA simulation efforts during the 70s and 80s were focused on simplified 2D geometries[5]. The research of welding heat source models dates back to Rosenthal works [6] who proposed a mathematical model of the moving heat source by concentrated heat point. Pavelic et al.[7] suggested a circular disc heat source model with Gaussian distribution of heat flux. Goldak et al.[8] further developed a double ellipsoidal power density distribution of heat source model below the welding arc, which can accurately simulate different types of welding processes with shallow and deep penetration. Recently, 3D welding simulation was conducted using commercial FEA software, as reported by Michaleris and DeBiccari[9], Brown[10], Dong et al.[11], and Chao et al.[12].

* Corresponding author: Tel./Fax: +98 9155107315.
E-mail address: mohsen.sh.1365@gmail.com

In this paper, residual stresses and distortion appeared in samples fixed by fixtures with three different size were investigated. For this purpose, gas tungsten arc welding (GTAW) of AA 5xxx aluminium alloy which used in ship structures, was analysed by ABAQUS general purpose finite element code[13]. Sequentially thermal mechanical method accompanied by double ellipsoid Goldak heat source model considered as analysis strategy. Heat losses by radiation and convection have been also taken into account. In order to reduce the number of elements, shell-to-solid coupling method has been utilized in the simulation. Parallel calculation analysis also applied in this simulation as an effective means to improve computing speed in finite element method.

Table 1 Chemical Composition

Alloys	Filler 5183	Base metal 5083
Si	0.25	0.14
Fe	0.40	0.25
CU	0.10	0.06
Mg	5.5	4.54
Mn	0.2	0.53
Pb	0.0008	4
Zi	0.10	1.4
Ti	0.2	0.02
Cr	0.2	0.11

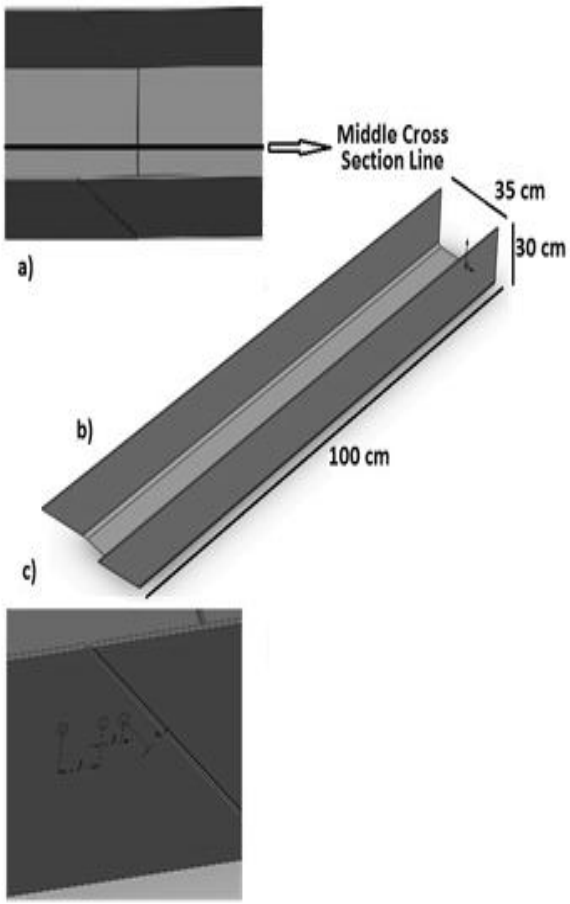

Fig. 1. Welding geometry: a) middle cross section line, b) part dimension, c) thermocouple situation

MATERIAL PROPERTIES AND GEOMETRY

AA 5083 aluminium alloy is the normal marine grade alloy used in the fabrication of passenger, freight and naval vessels. This alloy is preferred in nautical applications for its good weldability, strength and high corrosion resistance. Due to the demanding nature of the service conditions and environments in which marine vessels operate, welded components and structures are subjected to a high level of loads, which cause microstructural degradation and may finally lead to failure. The weld metal 5183 Al-alloy which is the most usual filler in combination with 5xxx alloys used as the filler. The chemical compositions of the two materials are reported in Table1.

Lap joint welding of two parts from an internal bridge used in the ship structure considered to be evaluated. Both parts are "U" shape and 1 meter long. Fig.1a and b illustrate type of joint and configuration details for this structure. These two parts (P1 and P2) have a precise primary dimension and should preserve their dimensional accuracy after welding. Because these parts are long, preserving their dimentional accuracy after welding is impossible and the parts experience some distortion. Therefore, it is necessary to control this distortion by some mechanical constraints, like fixtures. A Local U shape Fixture (LUF) has been utilized for this reason. This fixture excludes movement and keeps the two parts in proper position.

Figure 2. Shows the Local U shape Fixture (LUF) schematically. Welding parameters of GTA welding were the same in both sides of the bevel. These parameters summarized in Table2.After finishing the welding process, the resulting structure undergoes completing operation such as cutting, drilling and probably other welding processes.

In order to investigate the effect of LUF's length on the residual stresses and distortion, three sizes of L.U.Fs compared. The considered L.U.F's Lengths were 50 cm F1, 70 cm F2 and 100 cm F3. These fixtures had the same condition, except their length.

Welding sequence starts with putting two parts in the proper distance and installing LUF on the parts. Then, the inner region welds. Finally, L.U.F opens and the outer region welds.

Table 2. Welding parameters

Weld Region	Welding Method	Voltage	Amperage	Welding Coefficient	Shielded Gas
Outer and Inner Pass	GTAW	23 V	179 A	0.78	Ar 99%

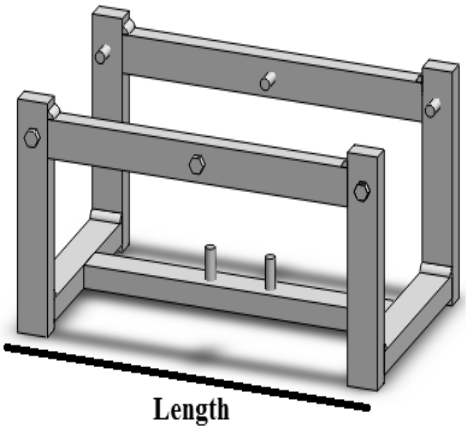

Name of L.U.F	Length
F1	50 cm
F2	70 cm
F3	100 cm

Fig. 2. Schematic of local U-shape fixture

Three K type thermocouples were mounted on the P1 cross sectional area at distances of 10, 20 and 40 mm from the weld center line to record the temperature history. The locations of thermocouples installation are shown in Fig. 1c. The thermocouples had 0.9 mm diameters and connected to a data acquisition device. Furthermore, linear variable displacement transducers (LVDT) were used during the experimental work in order to capture the out-of-plane distortion at the middle cross section line shown in Fig 1a.

Finite Element modelling

In this study, large complex welded structures have been analysed. There are several differences between parameters used in the current study and those usually utilized in the similar investigation. First, the length and number of weld lines are more than that usually in other simulations. second, the mesh at the weld positions were more complicated than those usually utilized in other traditional welding methods to capture the welding behaviour with greater accuracy. Third , the entire welded structure was simulated in this research, comprising 1 m in length of each part, which also increases the size of the finite element model. To overcome the problems of calculation capability and low efficiency of single PC's, parallel calculation technology was implemented by using an Ethernet cable connection directly between four computers.

Another useful technic helps decreasing computational time is application of shell elements in simulation. Shell elements are used to model structures in which one dimension, the thickness, is significantly smaller than the other dimensions. In this paper, a solid representation is used in the weld area to ensure more accurate capture of the high solution gradients. Because thermal gradients are not very large in the regions outside the welding zone, these regions modelled with shell elements to reduce the overall model size. The transition between the shell and solid regions is achieved using tied contact for the thermal analysis and shell-to-solid coupling for the stress analysis[13]. The mesh is shown in Fig.3.

An uncoupled thermal and mechanical analysis is adapted in this project. The thermal analysis was performed first and the transient temperature outputs from this analysis are saved for the subsequent thermo-mechanical analysis. It is assumed that deformations are sufficiently small for small deformation theory to be used throughout. The nodal temperatures are read from a results file generated during the thermal analysis and the mechanical analysis has the same number of steps as the thermal analyses. The FE mesh used in the mechanical analysis was the same as that used in the thermal analysis (see Fig. 3).

Thermal analysis

In the thermal analysis, the transient temperature field, T, is a function of time, t, and the spatial coordinates, (x, y, z) and is determined by the 3D nonlinear heat transfer equation (Eq. 1):

$$kT_{,ii} + Q_{int} = c\rho\dot{T} \quad (1)$$

Where k is the conductivity, Q_{int} is the internal heat source rate, c is the specific heat and ρ is the density of materials. The comma (,) denotes partial differentiation with respect to a spatial coordinate, the dot (.) denotes differentiation with respect to time, t.

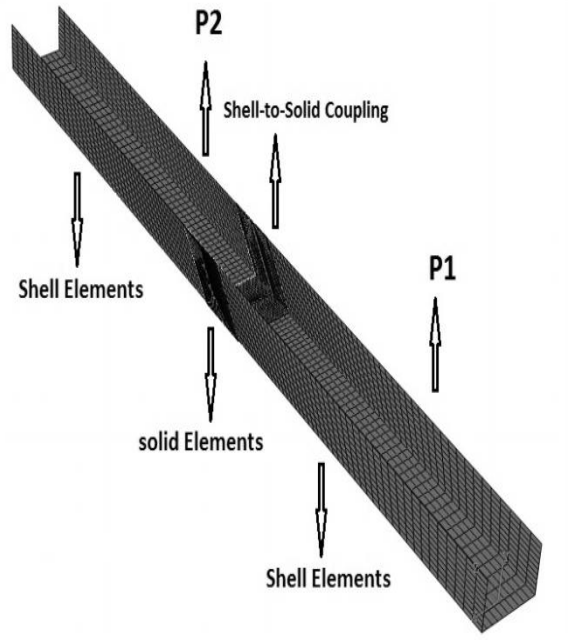

Fig. 3. Mesh structure based on shell-to-solid coupling

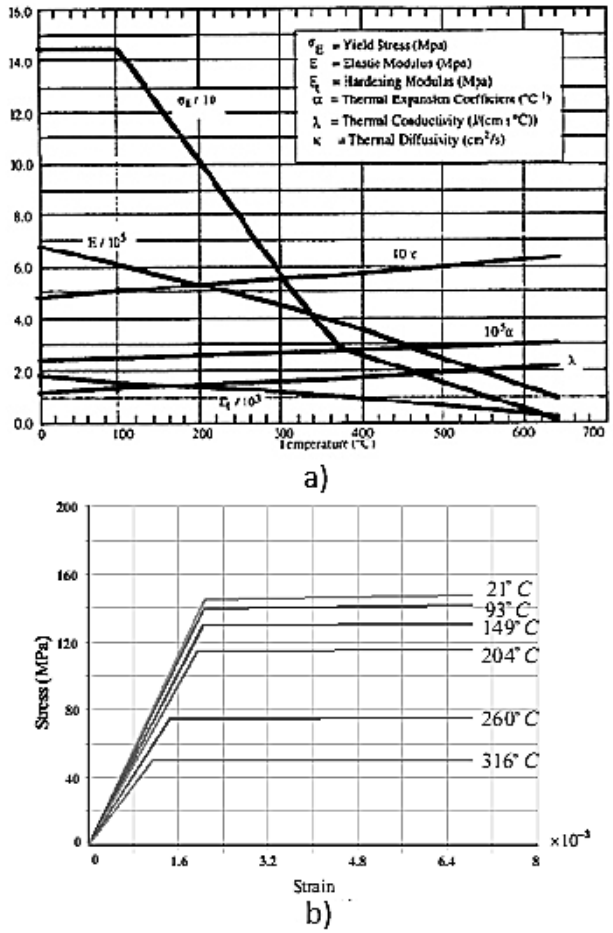

Fig. 4.a) Thermal and mechanical properties, and b) bilinear isotropic hardening model [14-15]

The inclusion of temperature-dependent thermo-physical properties along with a radiation term in the boundary condition makes this type of analysis highly nonlinear. However, the radiation heat exchange can be treated as convection, expressed by the following equivalent heat transfer coefficient (Eq. 2):

$$\tilde{h} = \frac{\varepsilon_{em}\sigma_{bol}((T+273)^4 - (T_{amb}+273)^4)}{(T-T_{amb})} + h_{con} \quad (2)$$

Where T_{amb} is the ambient temperature, $h_{con} = 30\ W/m^2{}^{\circ}C$ is the convection coefficient, $\varepsilon_{em} = 0.03$ is the emissivity of the plate surfaces[3] and $\sigma_{bol} = 5.67 \times 10^{-12}\ W/cm^2{}^{\circ}C$ is the Stefan–Boltzmann constant.

Heat loss by radiation and convection, were modelled in ABAQUS using the FILM subroutine. Latent heat of fusion considered to be 400 J/g for taking into the account the phase transformation of the aluminium[3]. Temperature-dependent AA 5083 thermal properties data required for welding simulation are shown in Fig. 4a[14-15]. Due to lack of filler material data, it is assumed that, thermal properties of the filler metal to be the same as those of the base metall.

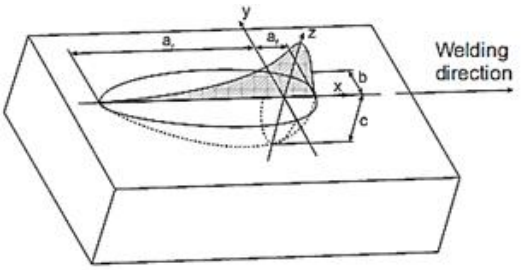

Fig. 5. Double ellipsoid Goldak model[8]

Heat source model

The physical phenomena associated with the interaction of the welding arc and the weld pool is complex and there are a number of models for describing the heat source of the weld torch. The Goldak ellipsoidal heat source model[8] utilized in this work, has been widely employed in the literature [16-18]. This model takes into account the heat which is transported below the surface when the weld bead is deposited. The ellipsoidal distribution is defined by the non-dimensional effective torch radius, r_e, which represents the distance from the torch centre (Eq. 3):

$$r_e = \sqrt{3(\frac{x-x_0}{a_f\ or\ a_r})^2 + 3(\frac{y-y_0}{b})^2 + 3(\frac{z-z_0}{c})^2} \quad (3)$$

The volumetric heat input, q , has a spatial variation based on this effective torch radius with its peak at the centre of the torch position.

$$q(x,y,z) = (f_f\ or f_r)q_{max}\exp^{-r_e^2} \quad (4)$$

In Eq. 3, x_0, $y_0$and z_0 give the torch position relative to the Cartesian axes and x, y and z represent the position where the heat flux is to be evaluated. Assuming an ellipsoid centred at (x_0,y_0, z_0) with semi-axes a, b, and c, as shown in Fig. 5, that the flux decays to 5% of the maximum value at the ellipse boundaries. The shape of the simulated heat flux is based on the weld bead profile measurement. Hence, $(a_f\ or\ a_r)$ is taken to be the distance from the weld bead start point to the weld torch centre in the front or rear of the arc center, 4.0 and 8.0 mm ; (b) is the half bead width, 3.0 mm, and (c) the bead height 2.5 mm.

As the heat input at different positions of the weld bead depends on the position of the weld torch as it travels along the centreline (x axis) with speed, v = 4.0 mm/s, the current position can be calculated according to the welding time, t. Thus Eq. 4 can be expressed on the following equations for taking into account the weld torch movement.

$$q_f(x,y,z) = q_{max}f_f e^{-3(\frac{x-x_0-vt}{a_f})^2} e^{-3(\frac{y-y_0}{b})^2} e^{-3(\frac{z-z_0}{c})^2} \quad (5)$$

$$q_r(x,y,z) = q_{max}f_r e^{-3(\frac{x-x_0-vt}{a_r})^2} e^{-3(\frac{y-y_0}{b})^2} e^{-3(\frac{z-z_0}{c})^2} \quad (6)$$

Where f_f *and* f_r are parameters which give the fractions of the heat transmitted in front and the rear parts of the weld, respectively. Note that $f_f + f_r = 2$, because the temperature gradient in the front leading part is steeper than that in the tailing edge.
The peak heat flux, q_{max} is:

$$q_{max} = \frac{6\sqrt{3}Q}{\pi\sqrt{\pi(abc)}} \quad (7)$$

In Eq. 7 Q is the energy input rate (J/s) which is given by the product of the heat input (J/mm), weld speed (mm/s) and the weld efficiency. The user subroutine DFLUX in ABAQUS[13] is used to introduce the body flux described by Eq. 5 and 6. The subroutine first calculates the position of the weld torch according to the welding time, t, then the heat flux, q, is computes at each integration point by the subroutine.

The initial temperature of the parent plate is set at room temperature (25˚c), but that of the weld bead is set to 600˚c. In fact, the initial temperature of the weld bead should also be set to room temperature and then allowed to reach its maximum temperature. However, numerical instabilities arose during the heating up of the weld bead, when combined with the incremental addition of the weld bead. Thus, in this analysis, an initial temperature of 600˚c was assigned to the weld bead and an associated initial heat flux, q, was included (see Eq. 1), which takes into account the heat flux required to heat the bead to 600˚c.

Mechanical analysis

In the thermo-mechanical analysis, the plastic deformation of materials is assumed to obey the Misses yield criterion and the associated flow rule. The rate relationship between thermal stresses, σ_{ij}, and strains, ε_{ij}, is described by Eq. 8:

$$\dot{\varepsilon}_{ij} = \frac{1+v}{E}\dot{\sigma}_{ij} - \frac{v}{E}\dot{\sigma}_{kk}\delta_{ij} + \lambda s_{ij} + [\alpha + \frac{\partial\alpha}{\partial T}(T - T_0)]\dot{T} \quad (8)$$

Where E is Young's modulus, v is Poisson ratio, α is the thermal expansion coefficient. $s_{ij} = \sigma_{ij} - (\frac{1}{3\sigma_{kk}\delta_{ij}})$ are the components of deviatoric stresses and λ is the plastic flow factor. $\lambda = 0$ for elastic deformation or $\sigma_e < \sigma_s$ and $\lambda > 0$ for plastic deformation or $\sigma_e \geq \sigma_s$, here σ_s is the yield stress and $\sigma_e = (3/2 s_{ij}s_{ij})^{1/2}$ is the Misses effective stress.

In this approach sections of the weld bead's elements are added incrementally to represent the transient nature of weld metal deposition. The stages of the analysis are as follows: stage 1: initially all bead elements are de-activated; stage 2: sections of the weld bead are re-activated (or borne) in successive steps to simulate weld metal deposition as the torch travels along the plate; stage 3: weld deposition is complete and the plate is allowed to return to room temperature.

In this work the *MODEL CHANGE option in ABAQUS was used to add and remove the weld bead elements. The length of the weld bead element sections added in each step is related to the size of the ellipsoidal heat flux distribution and the weld velocity.

Three different mechanical boundary conditions corresponding to three types of L.U.F's, i.e. F1, F2 and F3 used in the analysis for determining the best LUF size in welding sequence.

Mechanical properties of the weld material and parent plate are provided in Fig. 4a. Melting, solidification and annealing took into account in the analysis by ABAQUS command "ANNEAL TEMPERATURE". Using this command, a certain temperature defines such that the material lose its hardening history if the material temperature exceeds this certain temperature. The annealing temperature used is 500℃. Figure 4b shows the plastic deformations of the aluminum alloy 5083 at different temperatures which have been simulated using bilinear isotropic hardening model[15].

To reduce computational time, many numerical analyses often used a temperature above which no changes in the mechanical properties are accounted for[3]. A cut-off temperature of 400˚C (i.e. about 2/3 of the aluminum melting temperature) is used in the numerical calculations to reduce unnecessary computational time.

Experimental/analytical results and discussion

In this paper, a parallel calculation algorithm was performed for modelling of temperature field and distortion of a large complex welded structure during GTA welding. Parallel calculation is an effective means to improve computing speed in finite element analysis. Recently, with the rapid development of computer technology, parallel calculation implementation on high-performance personal computers (PCs) has attracted more attention and is now feasible.

The finite element model developed was calibrated using the experimentally measured thermal cycles as well as the shape and size of the weld zone determined by the macro-sections. Since the temperature histories for thermal analyses have the same values for all three types of L.U.Fs, the results of the thermal analysis have been used in all mechanical analysis on the inpute file. The temperature variation as a function of time, measured using thermocouples together with that obtained by simulation, illustrated in Fig. 6. As it's clear from the figure, there is a good agreement between experimental and simulated results.

For the sake of convenience in the following discussion, the middle cross-section of the model is defined as shown in Fig. 1a. is considered for reporting the distributions of computed values, such as stress and displacements, results. For comparison of experimental and FE model results, the vertical distortion values considered are those along a transverse section at half weld length location in middle cross-section line. Experimental vertical distortions have been measured using LVDT's installed on the middle cross-section line of the weld. The

measured and simulated values of vertical distortion summarized in Table 3.

As these values shown, the experimental and simulated results agree well in both the distortion tendency and distortion place of the structure. Moreover, trend of both simulated and experimentally determined distortion changes in the tree types of LUFs are same. Taking look at Table 3, it can be said thatis a small difference between experimentally determined and simulated distortion values.

The cause of this difference might be some simplifications made in the simulation. For example some experimental factors, such as heat input (Voltage, Current, Travel speed) are not pricesly controllable and their values may change slightly during the welding process.

The results of FEM show that, X axis distortion in F1 accrues near the welding region and this fixture type produces the most local and concentrated distortion with respect to the welding region.

The magnitude of distortion on the F2 was also more than the F3 type LUF; however these values are not critical.

Based on the results on the Table 3, during welding, presented the maximum distortion values related to welding according to 3 different types of LUFs. Based on the results on the table, during the welding if decrease of deformation is the purpose of using constraints, F1 type LUF satisfies this requirement.

Longitudinal and transvers residual stresses of three different types of LUFs illustrate in Fig.7. These Figures shows that although the distortion in F1 type LUF has the least value in the tree types of fixtures studied, the residual stress around the weld regions is high. This stresses exceed the critical values, i.e. the material yield stress. Therefore, occurrence of local plastic strains in welding region is highly probable. Such amounts of residual stresses cause to decrease the working life of structure in marine industries. Therefore, this type of LUF is not a suitable choice in the welding process.

In the F3 type of LUF, considerable amount of distortion observed on the areas far away the weld region. Distortion created after welding the inner side and removing the fixture, leads to mismatch problems in structure and dimensional correction on the process of production. However, the amount of residual stress is the least compared to two other LUFs. As result, in condition where removing the residual stress is the purpose, fixture type F3 is the more suitable choice.

In condition that both residual stress and distortion are significant and same importance during the producing structures, the LUF type F2 has better situation compared the other LUFs. However it is previously reported that, for only purpose of decreasing the residual stress or distortion, fixtures type F3 and F1 have the better condition respectively. For minimizing the residual stress in structure welded by fixture type F2, stress reliving using mechanical vibration or ultrasonic waves suggested. Otherwise, for decreasing the distortion on the both end sides of structure, primarily length can be designed longer and cutting the distorted pieces after the welding.

Table 3. Experimental and numerical level of distortion

LUF	Displacement (mm)			
	U_y		Location [a]	
	Exp.	Num.	Exp.	Num.
F1	From -4.0 To -5.6	-6.14	48	42
F2	From -7.0 To -9.52	-9.67	89	76
F3	From -9.5 To -11.5	-12.8	121	102

[a] Distance from weld centre line in the middle cross section line direction

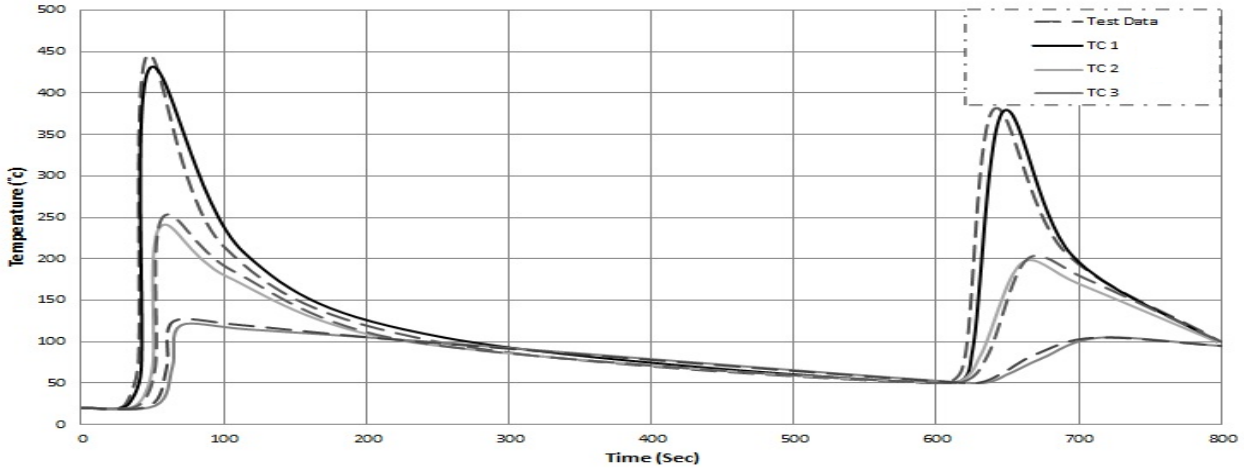

Fig.6 Thermal history, comparing Thermocouples and numerical results.

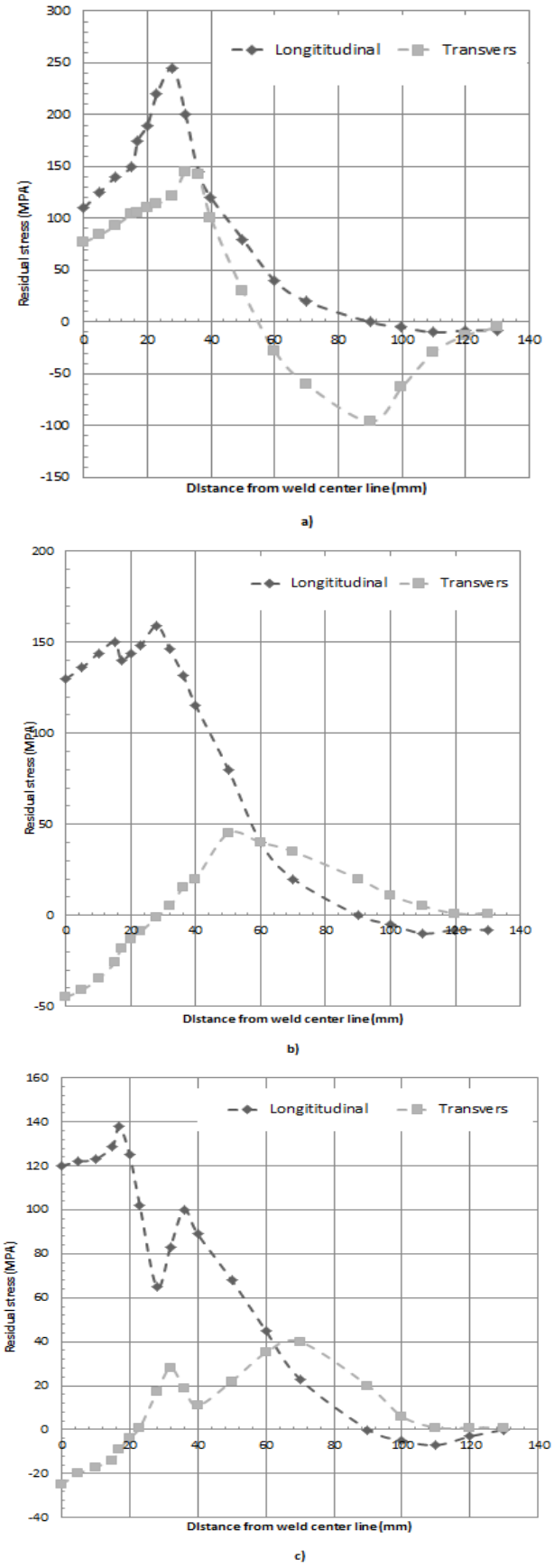

Fig.6 Transvers and longitudinal residual stresses along the middle cross section line. a) F1. b) F2. c) F3.

Conclusion

1- A parallel calculation algorithm was performed for modeling the GTA welding of 5XXX aluminum alloy.

2- Good agreement was achieved for the temperature field throughout the whole welding process.

3- Numerical results of distortion show proper match with experimental results extracted from installed LVDTs.

4- F1 is the best choose for designing a fixture in welding of the structure, if decreasing the deformation is the purpose during welding.

5- If removing the residual stress is the purpose, fixture type F3 is the more suitable choice.

6 -In condition that both residual stress and distortion are significant during the producing the structure, fixture type F2 has better situation compared the other FULs.

References

1. Sidhom, N., et al., Fatigue strength improvement of 5083 H11 Al-alloy T-welded joints by shot peening: experimental characterization and predictive approach. International Journal of Fatigue, 2005. 27(7): p. 729-745.
2. Yoon, J.W., et al., Buckling analysis for an integrally stiffened panel structure with a friction stir weld. Thin-Walled Structures, 2009. 47(12): p. 1608-1622.
3. Zhu, X.K. and Y.J. Chao, Effects of temperature-dependent material properties on welding simulation. Computers and Structures, 2002. 80: p. 967-976.
4. Hibbitt, H. D. and P. V. Marcal (1973). "A numerical, thermo-mechanical model for the welding and subsequent loading of a fabricated structure." Computers & Structures 3(5): 1145-1174.
5. Sherief, H. H. and M. N. Anwar (1986). "Two-Dimensional problem of a moving heated punch in generalized thermo elasticity." Journal of Thermal Stresses 9(4): 325-343.
6. Rosenthal, D., Mathematical theory of heat distribution during welding and cutting. Weld. J., 1941. 20: p. 220s-234s.
7. Pavelic, V., Tanbakuchi, R., Uyehara, O.A., Myers, P.S.,, Experimental and computed temperature histories in gas tungten-arc wwelding of thin plates. Weld. J., 1969. 48.
8. Goldak, J., Chakravarti, A., Bibby, M.,, A new finite element model for welding heat source.
. Metall. Trans. B, 1984(15): p. 299-305.
9. Michaleris P, D.A., Prediction of welding distortion. Weld J 1997. 76: p. 172s-81s.
10. Brown S, S.H., .Finite element simulation of welding of large structures. J Eng Ind, 1992. 114: p. 441-51.
11. Dong Y, H.J., Tsai CL, Dong P. , Finite element modeling of residual stresses in austenitic stainless steel pipe girth welds. Weld J, 1997. 76: p. 442s-9s.
12. Chao YJ, Z.X., Qi X. , WELDSIM—a welding simulation code for the determination of transient and residual temperature, stress and distortion. Advances in

Computational Engineering and Science, 2000. vol. II: p. 1206-11.
13. Hibbitt, ABAQUS/Standard User's Manual, (Pawtucket, USA, 1999).
14. Cañas, J., et al., A simplified numerical analysis of residual stresses in aluminum welded plates. Computers & Structures, 1996. 58(1): p. 59-69.
15. Hassanifard, S. and M. Zehsaz, The effects of residual stresses on the fatigue life of 5083-O aluminum alloy spot welded joints. Procedia Engineering, 2010. 2(1): p. 1077-1085.
16. Rieger, T., et al., Simulation of welding and distortion in ship building. Advanced Engineering Materials, 2010. 12(3): p. 153-157.
17. Kermanpur, A., M. Shamanian, and V.E. Yeganeh, Three-dimensional thermal simulation and experimental investigation of GTAW circumferentially butt-welded Incoloy 800 pipes. journal of materials processing technology 2008. 199: p. 295-303.
18. Shan, X., et al., Thermo-mechanical modelling of a single-bead-on-plate weld using the finite element method. International Journal of Pressure Vessels and Piping, 2009. 86(1): p. 110-121.